Hindawi
Journal of Nanomaterials
Volume 2020, Article ID 3672517, 12 pages
https://doi.org/10.1155/2020/3672517

Research Article

Effects of Boron Nitride Coatings at High Temperatures and Electromagnetic Wave Absorption Properties of Carbon Fiber-Based Magnetic Materials

Qilong Sun,[1,2] Wei Ye,[1,2] Jiahao Cheng,[1] and Xiaoyun Long[1,2]

[1]*National & Local Joint Engineering Research Center of Technical Fiber Composites for Safety and Protection, Nantong University, Nantong 226019, China*
[2]*College of Textiles and Clothing, Nantong University, Nantong, Nantong 226019, China*

Correspondence should be addressed to Wei Ye; 247173958@qq.com

Received 29 September 2019; Revised 11 December 2019; Accepted 4 January 2020; Published 20 January 2020

Academic Editor: Thathan Premkumar

An electromagnetic (EM) wave-absorbing material with a three-layer structure is prepared by depositing magnetic particles and a high-temperature resistant coating on the surface of the carbon fiber (CF) with in situ hybridization. Accordingly, the structure, chemical composition, morphology, high-temperature resistance, EM characteristics, and EM wave absorption of the composite materials were analyzed. The composite materials contained CFs, and the magnetic particles, such as Fe_3O_4, $NiFe_2O_4$, $CoFe_2O_4$, and Ni_3Fe, distributed along the axial direction of the fiber, while boron nitride (BN) existed in the outermost coating layer. This preparation method improves the oxidation resistance and EM wave absorption performance of the CF. When the concentrations of the metal salt solution and the original BN solution are 0.625×1.5 mol L^{-1} [$n(FeCl_3)$: $n(CoSO_4)$: $n(NiSO_4) = 2 : 2 : 1$] and 4 mol L^{-1} [$nH_3BO_3 : nCO(NH_2)_2 = 1 : 3$], respectively, the thermal decomposition temperature of the prepared CF/1.5FeCoNi/2BN is increased from 450°C to 754°C. In the frequency range of 10.6–26 GHz, the EM wave loss is less than −10 dB (the bandwidth spans 15.4 GHz). The CF-based composite material prepared in this study has the characteristics of light weight, wide absorption band, and strong oxidation resistance and constitutes the reference basis for the study of other high-temperature, EM wave-absorbing materials.

1. Introduction

When the aircraft travels through the air-intensive, low-altitude atmosphere, its surface temperature reaches several hundreds or even thousands of degrees Celsius within a short period of time [1]. Accordingly, at these temperatures, the absorbing materials on its structure cannot meet the radar requirements. Compared with graphite and spherical particles, carbon fiber (CF) has unique anisotropic characteristics, increased strength, and excellent thermal stability [2, 3]. It is not only extensively used in the reinforcing phase of composite materials, but it is one of the preferred materials for electromagnetic (EM) wave absorption. It is thus one of the preferred EM wave-absorbing materials, especially for high-temperature applications [4–7]. However, commercial carbon fiber exhibits metal-like properties, and its surface resistivity is low ($<10^{-5}$ Ω·m). It is a strong reflector of EM waves, so it must be structurally designed and chemically doped or surface modified to change the EM wave absorption performance of CFs [8].

Wei et al. [9] controlled the carbonization temperature to control the CF conductivity in the range of 10^{-3}–10^{3} Ω·m to prepare CFs that met the EM wave-absorbing requirements. Ishikawa [10] prepared a high-strength CF material with EM wave absorption and good electrical and magnetic properties based on the mixture of a magnetic metal powder, such as iron into a polyacrylonitrile spinning solution at a high Curie temperature, followed by its heating and carbonizing at temperatures in the range of 350–800°C. To date, many studies have been conducted on the direction of CF surface modification. Studies have shown that the introduction of metals, magnetic particles, high-molecular polymers, and

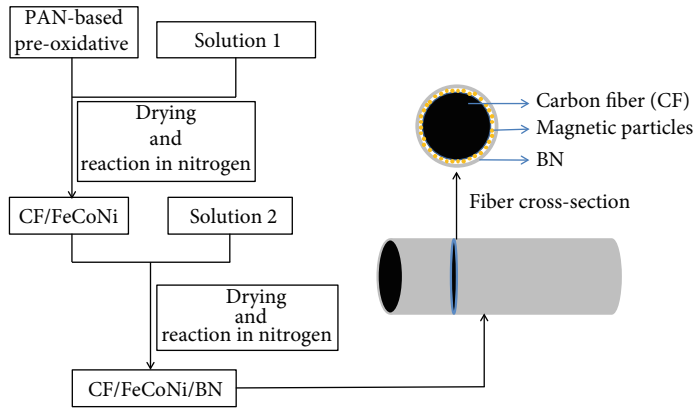

Figure 1: Preparation process for BN-coated high-temperature resistant material.

ceramic equivalents on the surface of the CFs can effectively improve the electromagnetic properties of carbon fibers [11–13]. If nickel and Fe_3O_4 are coated on the surface of the CF using electroless plating [14, 15], or if magnetic particles are formed on its surface in situ [16], the CF-based composite prepared by these surface modifications has an EM wave absorption performance that is superior to that of pure CF. Although various modifications of CF can improve the EM absorption properties of the material, the CF itself and the added metal and magnetic particles are exposed to air, especially in a high-temperature environment, thus making it susceptible to oxidation or corrosion. This limits its CF applications in high-temperature environments. Accordingly, depositing ceramic coatings on CF surfaces is an effective way to improve the material's high-temperature resistance and absorbing properties. Yan et al. used a one-step chemical vapor infiltration process to deposit silicon carbide (SiC) coating and SiC-C on the surface of CF [17], while Lii et al. used a dip coating that contained boric acid and a urea solution to form a boron nitride (BN) coating on the surface of the CF with high-temperature thermal decomposition [18]. All these methods can improve the high-temperature resistance and absorbing properties of CFs. Previous investigations have shown that boron in BN reacts with oxygen at temperatures above 900°C, forming B_2O_3 on the surface [19]. Therefore, by adjusting the loading of BN and magnetic particles, we can obtain materials with different electromagnetic wave absorption capabilities and oxidation resistance.

In this study, CF with dielectric loss is used as the inner layer, iron soft magnetic particles with magnetic loss are used as the intermediate layer, and the BN with high-temperature insulation and wave transmission properties is coated on the outermost layer of the CF. The traditional coating methods include electroplating, electroless plating, and reduction. However, these methods induce pollution in the environment during the production process. Conversely, the magnetic coating is difficult to diffuse into the fiber mat. In this study, a CF-based EM wave-absorbing material with a three-layer structure was prepared by a high-temperature heat treatment process.

2. Materials and Methods

2.1. Preparation of CF/FeCoNi/BN Composites. CF/magnetic particle/BN (CF/FeCoNi/BN) composites were prepared as illustrated in Figure 1. The typical procedure for the preparation of CF/FeCoNi/BN composites is as follows: (a) $FeCl_3$, $CoSO_4$, and $NiSO_4$ were supplied by Sinopharm Chemical Reagent Co., Ltd. Subsequently, $[n(FeCl_3): n(CoSO_4): n(NiSO_4) = 2 : 2 : 1]$ was dissolved in deionized water. (b) Polyacrylonitrile- (PAN-) based preoxidative felt (Nantong Sen Carbon Fiber Co., Ltd., fiber diameter of 1.5 dtex, 300 g/m^2) was then cleared, and the felt was added to solution 1 $[n\text{Fe} : n\text{Co} : n\text{Ni} = 2 : 2 : 1]$, whereby the rolling surplus rate was 600%. After drying, the PAN-based preoxidative fibers, which contained metal salts, were heat-treated at 650°C for 60 min in N_2 gas and covered the surface of the CF with a layer of magnetic particles. Finally, the resultant solution was mixed with solution 2 $[nH_3BO_3 : nCO(NH_2)_2 = 1 : 3]$ which contained three dip strands. The rolling ratio was 200%. The solution was then dried and treated at 500°C for 30 min. The prepared material was a three-layer CF matrix composite material (CF/FeCoNi/BN). CF/FeCoNi/BN was prepared with different metal salt solutions and different BN solutions. The BN compositions are given in Table 1.

2.2. Characterization. Phase structural analysis of the prepared CF/FeCoNi/BN was performed by X-ray diffraction (XRD, Rigaku D/max-2500PC) with CuKα radiation. A scanning electron microscope (SEM, Scios DualBeam) equipped with an energy dispersive spectrometer (EDS) was used for morphological observations and elemental analyses. The chemical compositions of the BN coating were analyzed by Fourier transform infrared spectroscopy (FT–IR, Nicolet iS10). The magnetic properties were achieved using a vibrating sample magnetometer (VSM; Quantum Design MPMS) at 300 K. The formation mechanism was analyzed by thermogravimetry/differential scanning calorimetry (TG/DSC, Netzsch 214 Polyma) at a heating rate of 5°C/min from 60°C to 1000°C in an argon atmosphere in the presence of air. The EM characteristics (relative complex permittivity

Table 1: Composition of the prepared composite samples with PAN-based preoxidative felt, $FeCl_3$, $CoSO_4$, $NiSO_4$, H_3BO_3, and $CO(NH_2)_2$.

Sample code	Base matrix (PAN-based preoxidative felt) quality (g)	Impregnation solution (mol L^{-1})				
		Solution 1			Solution 2	
		$FeCl_3$	$CoSO_4$	$NiSO_4$	H_3BO_3	$CO(NH_2)_2$
Carbon fiber (CF)	12	0.000	0.000	0.000	0.000	0.000
CF/1FeCoNi	12	0.250	0.250	0.125	0.000	0.000
CF/1.5FeCoNi	12	0.375	0.375	0.1875	0.000	0.000
CF/2.5FeCoNi	12	0.625	0.625	0.3125	0.000	0.000
CF/1FeCoNi/2BN	12	0.250	0.250	0.125	1.000	3.000
CF/2.5FeCoNi/2BN	12	0.625	0.625	0.3125	1.000	3.000
CF/1.5FeCoNi/1BN	12	0.375	0.375	0.1875	0.500	1.500
CF/1.5FeCoNi/2BN	12	0.375	0.375	0.1875	1.000	3.000
CF/1.5FeCoNi/3BN	12	0.375	0.375	0.1875	1.500	4.500

and relative complex permeability) were evaluated using a vector network analyzer (VNA; CeyearAV3672C) in the frequency range of 2.0-18.0 GHz. Before the test, the sample was thoroughly mixed with paraffin at a mass ratio of 3 : 7 and then pressed into a coaxial ring with outer and inner diameters of 7 and 3.04 mm, respectively. The reflection coefficient (RC) of the CF/FeCoNi/BN composite was determined in the frequency ranges of 8.2–12.4, 12–18, and 18–26 GHz, using the NRL arch method. A metal sheet (180 mm × 180 mm) and the CF/FeCoNi/BN composite with the same dimensions were successively placed on a sample platform, and two horn antennas were used to send and receive the EM wave normal to the sheet.

3. Results and Discussion

3.1. Crystal Structure. The crystal diffraction patterns of CF/1.5FeCoNi (without BN coating), CF/1.5FeCoNi/1BN, CF/1.5FeCoNi/2BN, and CF/1.5FeCoNi/3BN are shown in Figure 2. It should be noted that the PAN-based preoxidized fiber was impregnated with a metal salt solution and treated at 650°C, and soft magnetic particles, such as Fe_3O_4 (JCPDS 75-1609), $NiFe_2O_4$ (JCPDS 74-2081), $CoFe_2O_4$ (JCPDS 79-1744), and Ni_3Fe (JCPDS 88-1715), were formed by a series of thermal decomposition and reduction reactions at high temperatures. Subsequent immersion in a urea and boric acid mixture followed by a high-temperature treatment led to the formation of BN (JCPDS 45–0895) on the outermost layer of the CF. However, CF/1.5FeCoNi/1BN did not show significant (002) and (100) plane diffraction peaks at 26.5° and 43.3°. The main reason was attributed to the fact that the positions of 21.6° and 43.3° are typical CF diffraction peaks [20], while the position at 43.3° is also a strong diffraction peak of Fe_3O_4, $NiFe_2O_4$, and $CoFe_2O_4$. As the BN content increased, the peak near 26.5° becomes sharper. At the same time, the typical peaks of Fe_3O_4, $NiFe_2O_4$, $CoFe_2O_4$, and Ni_3Fe did not disappear, indicating that the coverage of BN did not affect the existence of magnetic particles.

3.2. Infrared Analyses. The infrared (IR) spectra of the CFs that were coated with different BN concentrations are shown

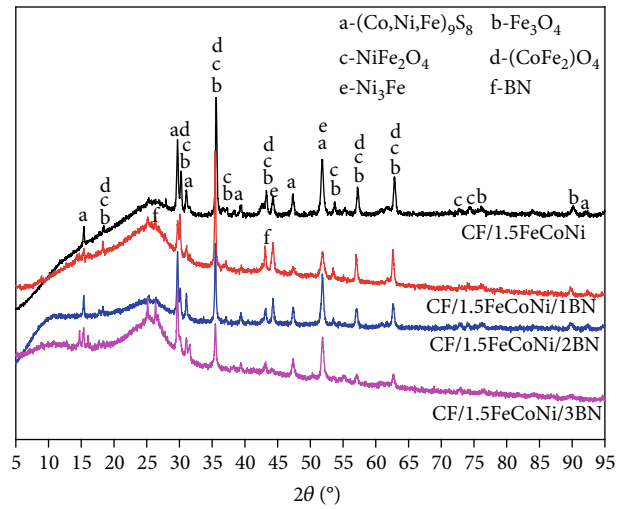

Figure 2: X-ray diffraction (XRD) profiles of carbon fiber (CF)/1.5FeCoNi, CF/1.5FeCoNi/1BN, CF/1.5FeCoNi/2BN, and CF/1.5FeCoNi/3BN.

in Figure 3, and the IR spectrum of the uncoated CFs is also shown for comparison. The CF impregnated with the mixed solution of urea and boric acid has absorption peaks at 780 and 1380 cm^{-1} after high-temperature treatment, which correspond to B-N in-plane stretching and B-N-B out-of-plane bending [18, 21], respectively. The O-H band in the range of 2800–3600 cm^{-1}, the C-N band at 1023 and 1190 cm^{-1}, and the absorption peak became more obvious as the original BN solution concentration increased. This means that despite the high-temperature treatment, some of the urea and boric acid are not completely decomposed. This may be attributed to the insufficient processing time or processing temperature. The IR spectroscopy results were consistent with those obtained from the XRD analyses. It can be observed that there is a BN coating on the outermost surface of the prepared CF-based composite.

3.3. Morphological Analyses. The surface topography of the material is shown in Figure 4. It can be observed that the prepared composite material has magnetic properties because

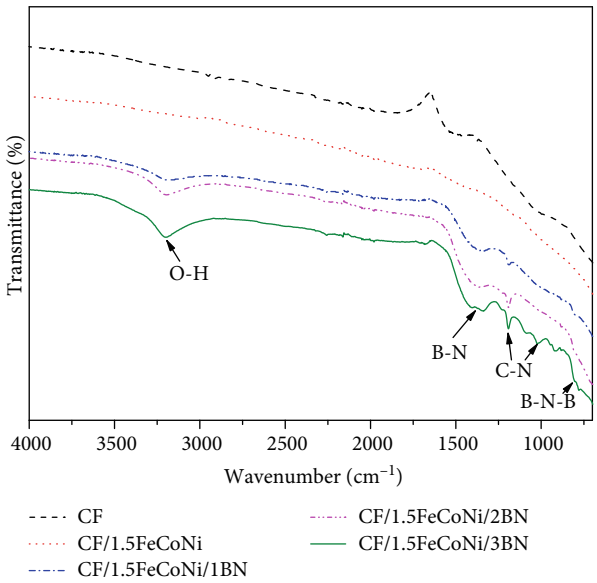

Figure 3: FT–IR spectra of CF, CF/1.5FeCoNi, CF/1.5FeCoNi/1BN, CF/1.5FeCoNi/2BN, and CF/1.5FeCoNi/3BN.

the fiber surface covers a large number of magnetic particles with magnetic loss properties. At the same time, after the PAN-based preoxidized silk was finished by the metal salt and the BN source solution, the magnetic particle and the BN coating layers appeared in succession on the surface of the fiber. After the deposition of the BN coating, a film was formed on the surface of the CF. This film enhances the heat resistance of the material and may also enhance the absorbing properties of the material in certain conditions [22]. The surface of the CF that is not covered with the BN coating contains no film, and only the magnetic particles are distributed. After the metal salt is impregnated, the surface of the fiber is uniformly distributed with magnetic particles, and the larger the concentration of the metal salt is, the larger are the magnetic particles [16]. The concentration of boric acid is different, and the surface morphology of the CF is also different. The thicker the BN concentration is, the thicker the film covering on the surface of the CF is. When the concentration of boric acid is 1.5 mol L^{-1}, needles are formed on the surface of CF, and the surface coating of the fiber appears. Based on the analyzed results, it is inferred that after the high-temperature carbonization has covered the BN coating, all the fibers maintain their surface topographies and microstructural properties. At the same time, there are many protrusions on the surface of the fiber, and the density is relatively large and evenly distributed. These large-area protrusions help increase the interfacial effect and strengthen the fiber's ability to absorb EM waves [23]. The uniform distribution of magnetic particles and BN on the surface of the fiber is beneficial in maintaining the stability and improving the oxidation and corrosion resistances of the material. Furthermore, there is a gap between fibers, which is beneficial for the penetration of the EM in the material and for the reduction of the loss caused by the EM in the material.

3.4. EDS Analyses. Figure 5 shows the EDS elemental analysis of the fiber surface. We can clearly see the presence of B, N, C, Fe, Co, Ni, and other elements on the surface of the CF. These elements are important components of magnetic particles and BN. Figure 6 shows a scanning view of the element surface of CF/1.5FeCoNi/2BN. It can be observed that B, N, C, Fe, Co, and Ni are uniformly distributed on the surface of the fiber. B and N constitute a high-temperature resistant BN coating, which can increase the oxidation resistance temperature of the CF, reduce the surface resistance of CF, and reduce the reflection of EM by fibers. At the same time, the surface of the fiber is evenly distributed with soft magnetic particles composed of elements, such as Fe, Co, and Ni. These magnetic particles have obvious absorbing properties and are commonly used for electromagnetic wave absorption [15, 16]. Additionally, various EM-absorbing materials form a special structure on the surface of the fiber and have a rich interfacial polarization that is beneficial to the improvement of the EM wave absorption performance of the material.

3.5. Magnetic Hysteresis Analyses. The magnetic behaviors of CF and CF/1.5FeCoNi/2BN composites were analyzed by VSM analysis at room temperature. Figure 7 shows that the hysteresis loop of the initial CF is almost a straight line, which indicates nonmagnetic behavior, while the hysteresis loop of the CF/1.5FeCoNi/2BN is a typical S-type curve. As shown in Figure 7. The saturation magnetization (M_s), remnant magnetization (M_r), and coercive force (H_C) of the CF/1.5FeCoNi/2BN composites obtained at room temperature are 15.47 emu/g, 5.55 emu/g, and 2006.4 Oe, respectively. The difference in magnetic properties of these two composites maybe attributed to the introduction of magnetic Fe_3O_4, $NiFe_2O_4$, and $CoFe_2O_4$.

3.6. Thermal Analyses. Figure 8 shows the TG and DTG curves of the boric acid and urea mixture in the presence of N_2. When the temperature is approximately 94.5°C, the boric acid undergoes dehydration to form $H_2B_4O_7$ [24]. When the temperature is approximately 180°C, a fast loss of weight is documented that is attributed to the condensation and hydrolysis reactions of urea that release a large amount of NH_3 [25]. When the temperature reaches ~304.5°C, the boric acid is completely dehydrated to form B_2O_3 and H_2O. As the temperature is further increased, B_2O_3 and NH_3 react to form BN. The reaction equations that describe the entire process are given below:

$$4H_3BO_3 \longrightarrow^{\Delta,N_2} H_2B_4O_7 + 5H_2O\uparrow \quad (1)$$

$$CO(NH_2)_2 + H_2O \longrightarrow^{\Delta,N_2} 2NH_3\uparrow + CO_2\uparrow \quad (2)$$

$$H_2B_4O_7 \longrightarrow^{\Delta,N_2} 2B_2O_3 + H_2O\uparrow \quad (3)$$

$$B_2O_3 + 2NH_3 \longrightarrow^{\Delta,N_2} 2BN + 3H_2O\uparrow \quad (4)$$

Figure 9 shows the TG and DTG curves of different materials in the presence of air. We can observe that pure CF begins to oxidize and decompose in air at 450°C and is completely oxidized at 670°C. At the same time, we found that the thermal decomposition temperature of CF decreased

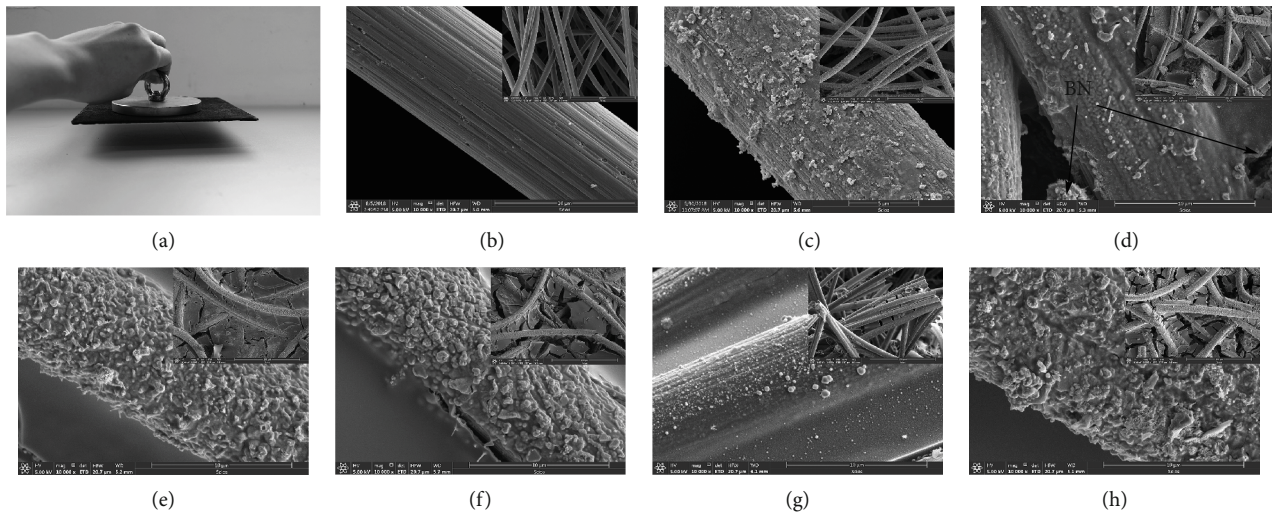

Figure 4: Scanning electron microscopy (SEM) images showing the (a) magnetic performance, (b) CF, (c) CF/1.5FeCoNi, (d) CF/1.5FeCoNi/1BN, (e) CF/1.5FeCoNi/2BN, (f) CF/1.5FeCoNi/3BN, (g) CF/1FeCoNi/2BN, and (h) CF/2.5FeCoNi/2BN.

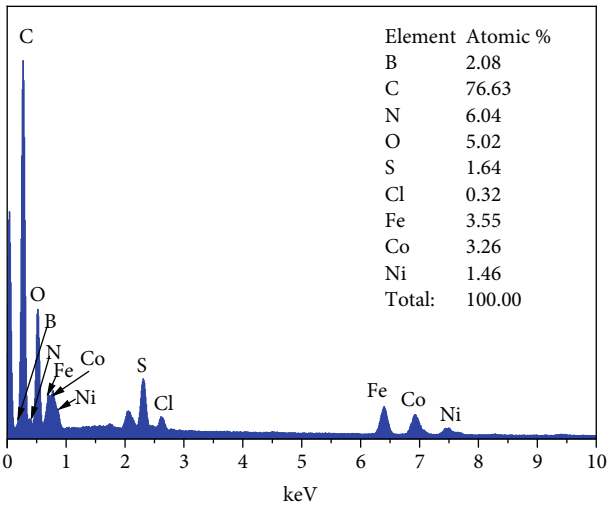

Figure 5: Energy dispersive spectrometer (EDS) outcomes of CF/1.5FeCoNi/2BN.

after it was covered with soft magnetic particles. This is because the presence of metal ions catalyzes the oxidation of CFs [26]. When BN is deposited, the thermal decomposition temperature of the CF-based EM wave-absorbing material is remarkably improved. We can observe that there are multiple decomposition temperatures in the thermal decomposition curve of the material after the BN deposition. Because of the 30 min treatment at 500°C, the urea and boric acid decomposition was partially incomplete. Based on IR analyses, it can be observed that the two compounds are not completely decomposed. Therefore, it is considered that the last decomposition temperature region is the temperature at which the CF actually begins to decompose. When the concentration of the BN stock solution is equal to unity ($nH_3BO_3 = 0.5\,\text{mol}\,L^{-1}$ and $nCO(NH_2)_2 = 1.5\,\text{mol}\,L^{-1}$), the decomposition temperature appears to be approximately equal to 622°C. This is because the concentration is low, which results in an insufficient BN thickness and coverage area on the fiber surface, and ultimately leads to a low-thermal decomposition temperature. Further increase of the impregnation concentration can increase the coverage of BN and thus lead to an increased decomposition temperature. As it can be observed from the figure, when the concentration increases by a factor of two to three, the decomposition temperature is increased to 754°C and 804°C, respectively. This is because when the concentration becomes high, the BN content of the outermost layer of the fiber increases, which enhances the oxidation resistance. Even though the temperature rises to 650–1000°C, BN begins to oxidize and eventually fails, but the B_2O_3 film formed by BN oxidation can act as a barrier to prevent oxygen permeation [27] and thus delays the oxidation rate of the fiber. These findings show that after the modification of BN coating, the initial and final oxidation temperatures and the oxidation resistance of the material are all improved.

3.7. EM Characteristics. Figures 10(a), 10(b), 10(d), and 10(e) show the measured complex permittivity and permeability in the range of 2–18 GHz for nine samples comprising 30 wt% CF, CF/1FeCoNi, CF/1.5FeCoNi, CF/2.5FeCoNi, CF/1FeCoNi/2BN, CF/2FeCoNi/2BN, CF/1.5FeCoNi/BN, CF/1.5FeCoNi/2BN, and CF/1.5FeCoNi/3BN composites. There are two possible contributions to microwave absorption: dielectric loss and magnetic loss. We have also calculated the dielectric tangent loss ($\tan \delta e = \varepsilon''/\varepsilon'$) and magnetic tangent loss ($\tan \delta m = \mu''/\mu'$) based on the permeability and permittivity of samples measured as described above, shown in Figures 10(c) and 10(f). From Figures 10(a) and 10(b), we can find that the values of ε' and ε'' of the CF/1FeCoNi, CF/1.5FeCoNi, and CF/2.5FeCoNi samples are stable in the range of 2–18 GHz; the values are approximately 3.5 and 0.3, respectively. This shows that the material has no obvious relaxation and resonance behavior in the entire dielectric spectrum, and the dipole orientation polarization may be the main

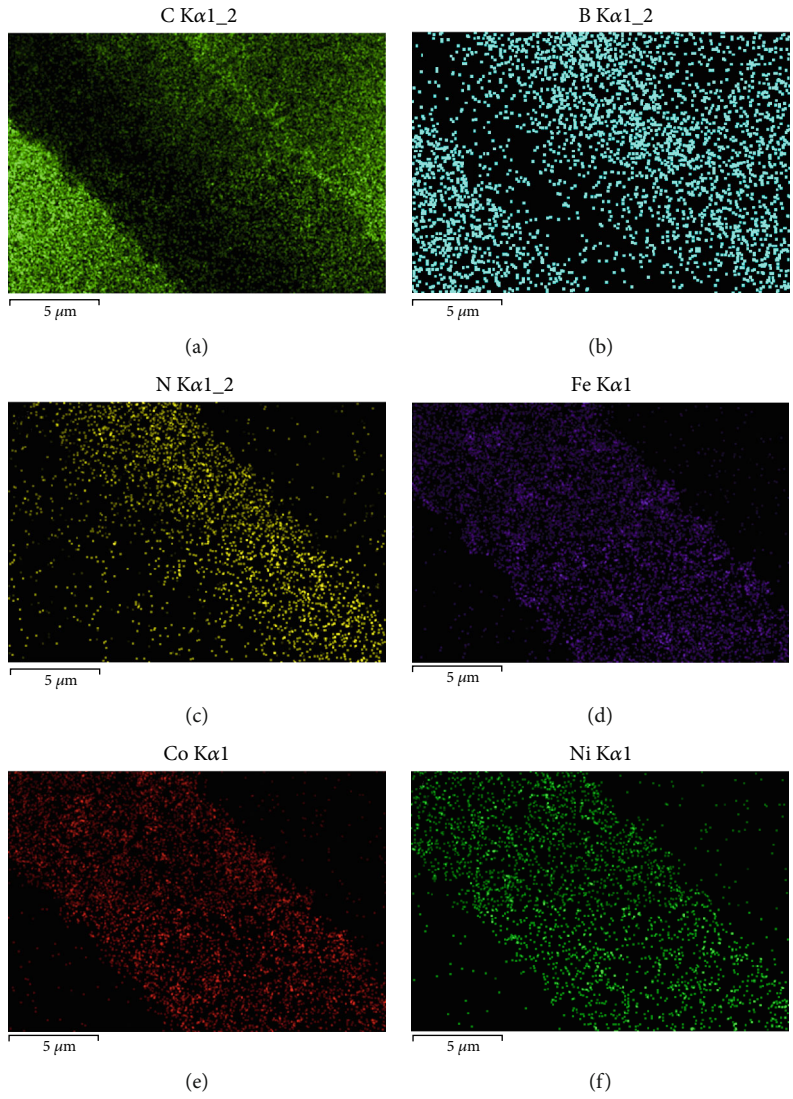

Figure 6: SEM topography maps of CF/1.5FeCoNi/2BN composites for elements (a) C, (b) B, (c) N, (d) Fe, (e) Co, and (f) Ni.

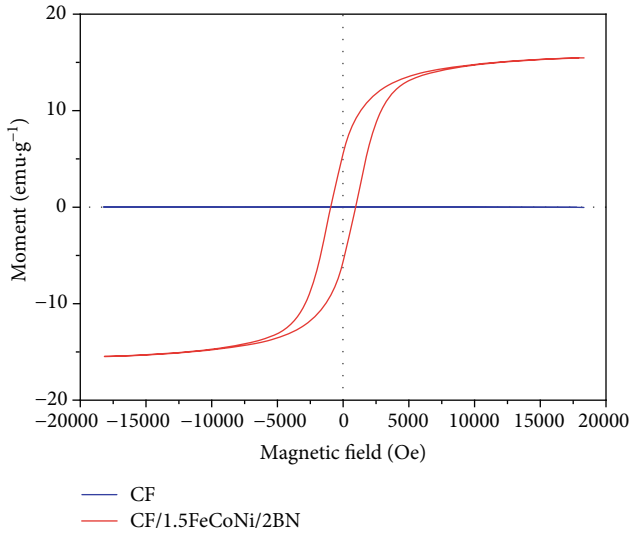

Figure 7: Magnetic hysteresis loops of CF and CF/1.5FeCoNi/2BN.

polarization mechanism in this frequency range [28]. The outer layer of the magnetic particles is combined with the BN layer, and ε' of CF/1FeCoNi/2BN, CF/2.5FeCoNi/2BN, CF/1.5FeCoNi/1BN, CF/1.5FeCoNi/2BN, and CF/1.5FeCoNi/3BN becomes smaller because BN is a high-resistance electromagnetic wave-absorbing material [29], so the surface resistance of carbon fiber-based magnetic fibers decreases, and ε' also decreases. From the curve of ε'', we observe that there is a broad dielectric resonance peak around 10 GHz, and there is a significant dielectric relaxation phenomenon [30]. In comparison with the ε'' values of some other carbon/magnetic composite materials [31–33], the value of ε'' is too small. Thus, it can be inferred that the prepared material has higher resistance. The reason for this may be that the BN resistance is high, and the resulting composite material has fewer defects. In general, a suitable resistance and dielectric loss are beneficial for improving the electromagnetic wave absorption performance of the material. From Figures 9(d) and 9(e), we can observe that the curves

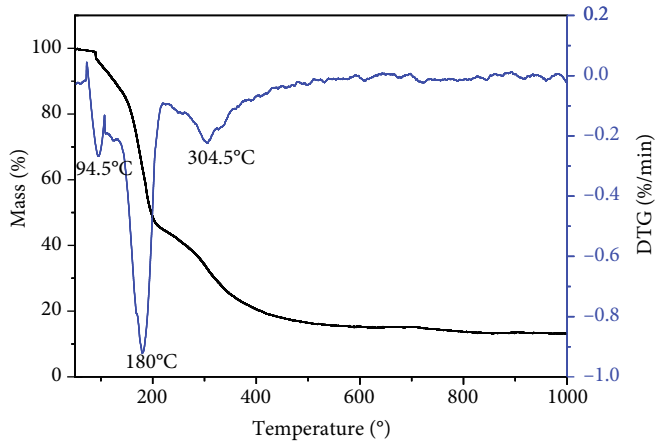

Figure 8: Thermogravimetry (TG) and derivative thermogravimetric (DTG) curves of boric acid and urea.

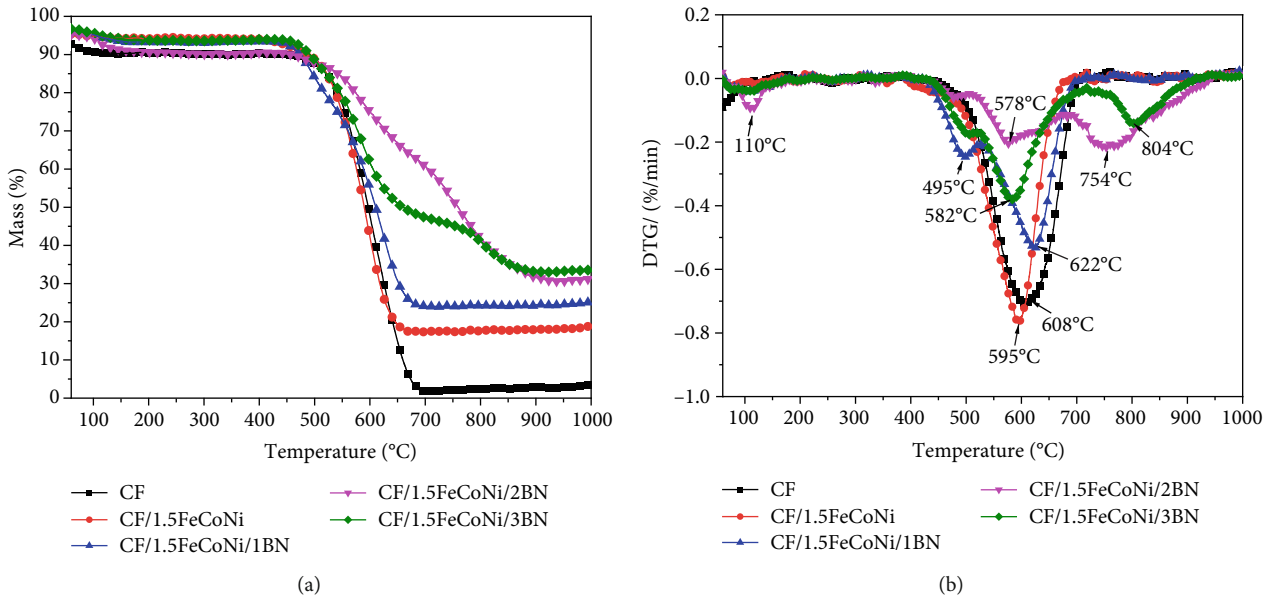

Figure 9: TG (a) and DTG (b) curves of CF, CF/1.5FeCoNi, CF/1.5FeCoNi/1BN, CF/1.5FeCoNi/2BN, and CF/1.5FeCoNi/3BN.

of μ' and μ'' of the uncoated BN magnetic fiber composite materials show little fluctuation, and their values are around 1 and 0, which is consistent with the description in the literature [34]. Another report similarly indicated that magnetic loss of the carbon magnetic composite material is not a key factor for its electromagnetic absorption performance [35]. Because of the addition of BN, the values of μ' and μ'' of carbon magnetic materials have increased significantly, indicating that the presence of BN enhances the magnetic loss performance of the material, which is a very interesting phenomenon. Furthermore, an obvious magnetic resonance peak appeared near 12 GHz, which is due to the surface effect and spin wave excitation of magnetic particles [36]. The dielectric loss tangent and magnetic loss tangent can characterize the dielectric loss and magnetic loss of the material, respectively. The dielectric loss and magnetic loss are two main mechanisms whereby materials absorb electromagnetic waves. To determine the dominant mechanism in the material, we calculated the tan δe and tan δm of each sample. The results are shown in Figures 10(c) and 10(f). We found that for materials covered only with magnetic particles, tan δe of CF/1FeCoNi is approximately 0.2, the other materials are at 0 attachments, and tan δm of carbon magnetic materials is essentially 0. However, after covering BN, both tan δe and tan δm in the sample can reach a certain value; for example, tan δe of CF/1.5FeCoNi/2BN is between 0.1 and 0.35, and tan δm is between 0.2 and 1. The existence of BN shows that the electromagnetic absorption of the prepared carbon magnetic material has both dielectric loss and magnetic loss. However, in practical applications of electromagnetic wave-absorbing materials, impedance matching, electromagnetic loss synergy, and the three-dimensional structure of the material can greatly affect the electromagnetic wave absorption performance of the material [34, 37, 38].

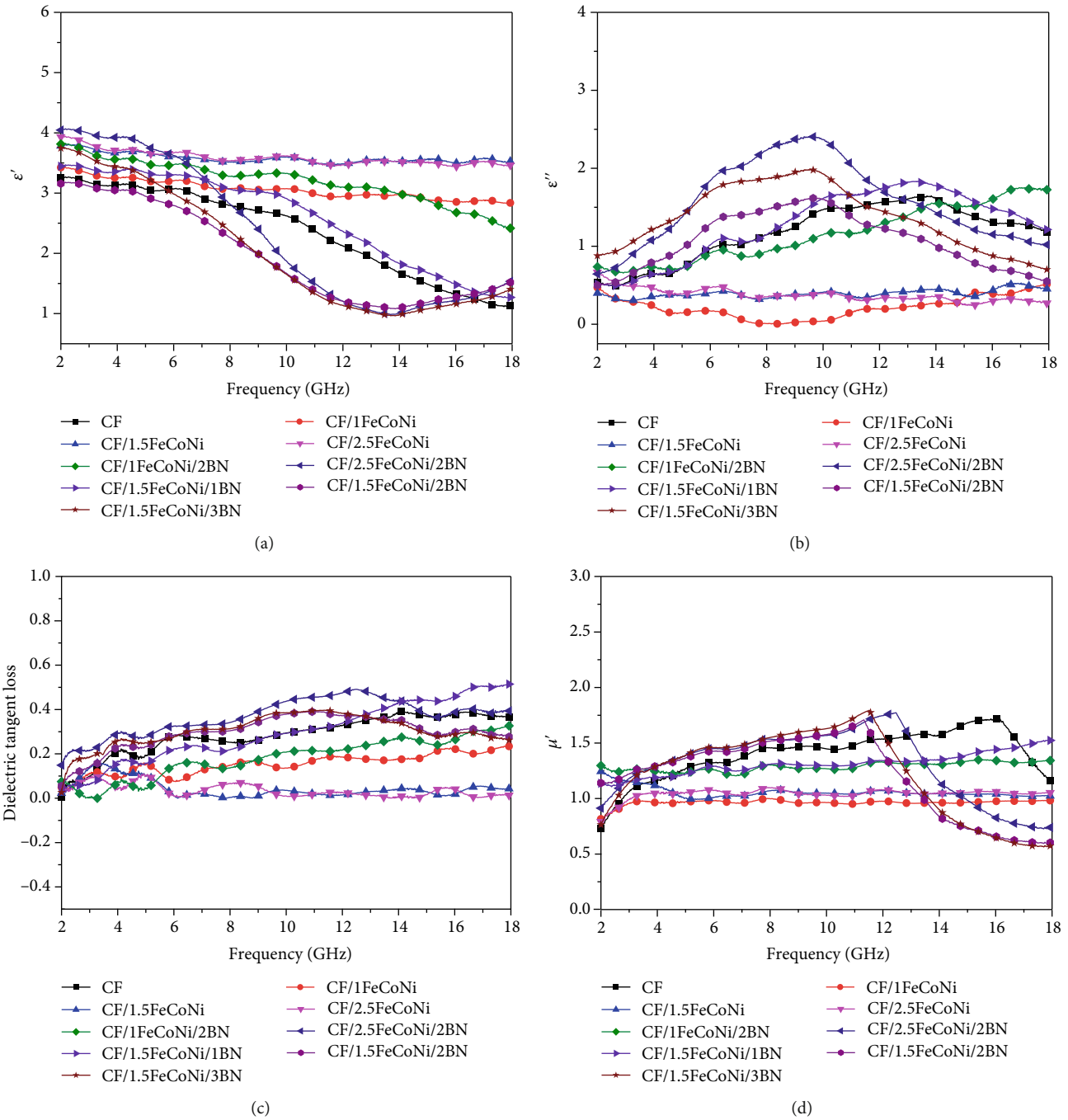

Figure 10: Continued.

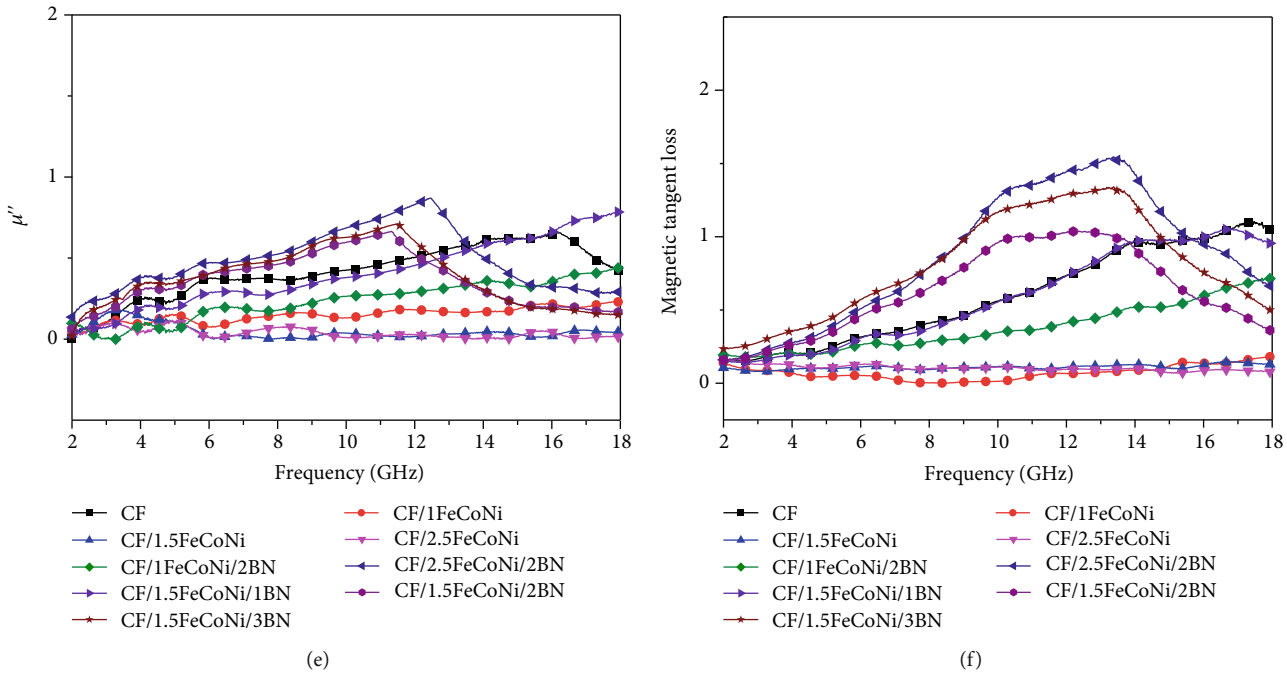

FIGURE 10: Frequency dependence on real (a) and imaginary (b) parts of the complex permittivity of samples, real (d) and imaginary (e) parts of the complex permeability, and the corresponding dielectric (c) and magnetic (f) loss tangents of CF, CF/1FeCoNi, CF/1.5FeCoNi, CF/2.5FeCoNi, CF/1FeCoNi/2BN, CF/2FeCoNi/2BN, CF/1.5FeCoNi/BN, CF/1.5FeCoNi/2BN, and CF/1.5FeCoNi/3BN composites.

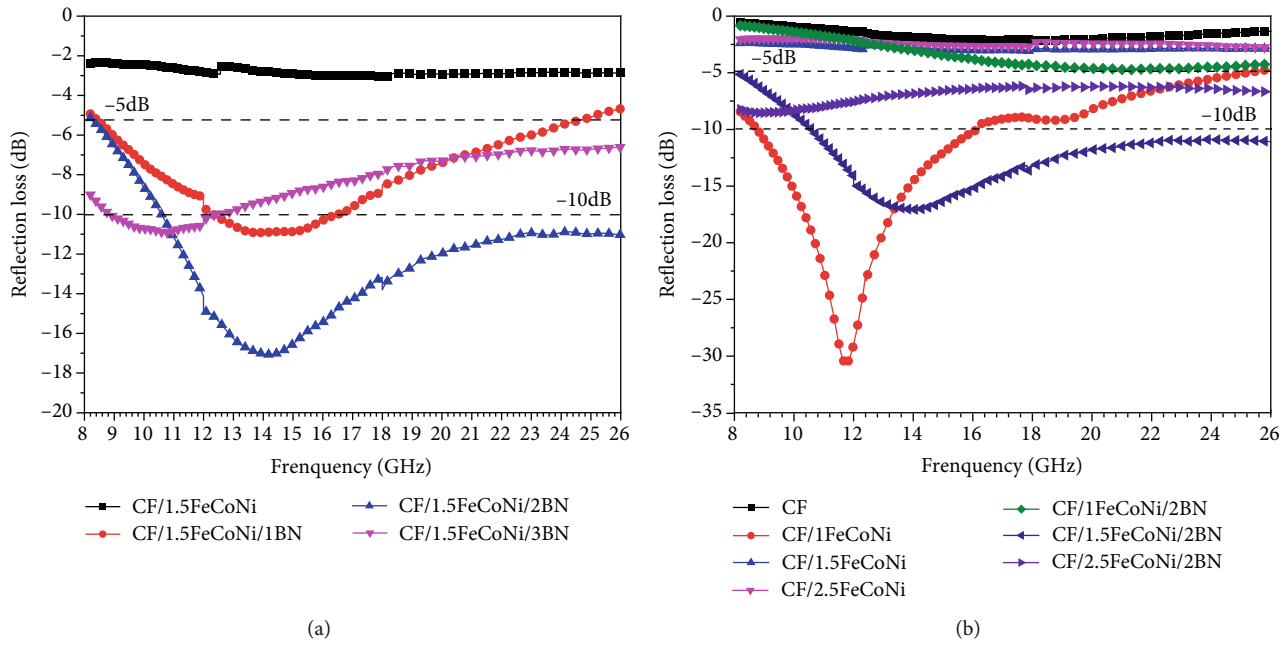

FIGURE 11: EM wave absorption properties (a, b) of materials prepared at different conditions.

3.8. EM Wave-Absorbing Properties. Figure 11 shows the EM wave absorption curve of CF matrix composites. We can infer that the loading of the magnetic particles on the surface of CF affects the EM wave absorption performance of the material. When the concentration of the metal solution is 0.625 mol L^{-1}, the electromagnetic wave loss of the material within the 8.7–16.1 GHz band is less than -10 dB, and the lowest loss is −30.62 dB. As the concentration of metal salt increases, the EM wave absorption performance of the material diminished. This is attributed to the fact that when the concentration is increased, magnetic particles on the surface of the fiber become larger. This affects the EM wave absorption performance [12], thus causing the alloy on the surface of the fiber to increase, which leads to the

formation of a conductive network between the fibers. The EM wave absorption performance is thus weakened [39]. At the same time, the EM wave absorption performance of the material can be optimized after the outermost layer of the magnetic particles is covered with BN. We found that CF/1.5FeCoNi/2BN has an electromagnetic wave loss <−10 dB (bandwidth of 15.4 GHz) in the frequency range of 10.6–26 GHz. This is attributed to the fact that when BN is deposited, there is a contact between the fibers and BN, fibers and magnetic particles, and magnetic particles and BN, which creates a large number of interfacial effects and produces more interfacial polarization [23]. In addition, BN is a high-resistance material that can affect the formation of conductive networks and reduce the reflection of EM waves. When the dielectric loss, magnetic loss, and material structure work together, the EM wave absorption properties of the material can be enhanced [40, 41]. At the same time, we found that when the loading of magnetic particles and the thickness of BN coating changed, the EM wave absorption properties of the material also changed. We found that when the BN preparation solubility increased by a factor of two, the EM wave absorption performance first increased and then decreased as the concentration of the metal salt increased. This was because the BN resistance was large, and the fiber dielectric loss, interface effect between the magnetic particles and the CF, and electronic transition were all changed after the fiber surface was covered. When the content of soft magnetic particles was small, the original electronic transition network and interface polarization effects were affected and changed, and the EM wave absorption performance also changed. When the metal salt concentration was high, the magnetic particles supported on the fiber surface became larger. An excessive number of magnetic particles make the EM wave absorption process ineffective [16]. Similarly, the variation of the thickness of the BN coating on the surface of CF also affected the EM wave-absorbing composites in which the three-dimensional network structure and various lossy materials worked synergistically. Based on the above considerations, the influencing mechanism requires further study.

4. Conclusions

In this study, PAN-based CF was selected as the substrate, and its high-temperature resistance, oxidation resistance, high strength, and light weight were fully utilized to yield good EM wave absorption performance and a strong corrosion resistance. The magnetic particles were supported on the surface of the CF by in situ hybridization, and the outermost layer was coated with a high-temperature resistant BN. A three-layer CF-based, high-temperature, EM wave-absorbing material with light weight and a broad absorption response was prepared. This special structure mediated electrical loss, magnetic loss, and three-dimensional network synergy that enhanced the material's EM wave absorption performance. The prepared CF/1.5FeCoNi/2BN had an absorption bandwidth of 15.4 GHz (10.6–26 GHz) with a reflection loss that exceeded −10 dB. At the same time, the presence of BN significantly improved the oxidation resistance of CFs. The CF/1.5FeCoNi/2BN sample began to decompose at approximately 754°C, which increased the thermal decomposition temperature of the CF by 304°C. From the perspective of a comprehensive performance, the CF/FeCoNi/BN composite absorbing materials have the potential to become new types of high-temperature absorbing composite materials with excellent response characteristics, including broadband, high efficiency, stability, and light weight.

Abbreviations

EM: Electromagnetic
BN: Boron nitride
CF: Carbon fiber
DSC: Differential scanning calorimetry
EDS: Energy dispersive spectrometer
FT–IR: Fourier transform infrared spectroscopy
IR: Infrared
RC: Reflection coefficient
SEM: Scanning electron microscope
TG: Thermogravimetry
XRD: X-ray diffraction.

Data Availability

The data used to support the findings of this study are available from the corresponding author upon request.

Conflicts of Interest

The authors declare that they have no conflicts of interest.

Acknowledgments

This study was supported by the National Key Research and Development Program of China (2016YFB0303100 and 2018YFC0810300), a project funded by the Priority Academic Program Development of Jiangsu Higher Education Institutions (Su Caijiao [2018] No. 192), and the National Science Foundation for Young Scientists of China (Grant No. 51503105).

References

[1] C. H. Zhang, "Surface heating temperature caculation of landed missile heavy wall aerodynamic," *Journal of Shenyang Institute of Aeronautical Engineering*, vol. 27, no. 1, pp. 14–17, 2010.

[2] T. Han, H. Wang, X. Jin et al., "Multiscale carbon nanosphere–carbon fiber reinforcement for cement-based composites with enhanced high-temperature resistance," *Journal of Materials Science*, vol. 50, no. 5, pp. 2038–2048, 2015.

[3] S. Tang and C. Hu, "Design, preparation and properties of carbon fiber reinforced ultra-high temperature ceramic composites for aerospace applications: a review," *Journal of Materials Science & Technology*, vol. 33, no. 2, pp. 117–130, 2017.

[4] K. Osouli-Bostanabad, H. Aghajani, E. Hosseinzade, H. Maleki-Ghaleh, and M. Shakeri, "High microwave absorption of nano-Fe3O4 deposited electrophoretically on carbon fiber," *Advanced Manufacturing Processes*, vol. 31, no. 10, pp. 1351–1356, 2015.

[5] F. D. Ning, W. L. Cong, J. J. Qiu, J. H. Wei, and S. R. Wang, "Additive manufacturing of carbon fiber reinforced thermoplastic composites using fused deposition modeling," *Composites Part B Engineering*, vol. 80, pp. 369–378, 2015.

[6] X. Liu, R. Wang, W. Liu, Y. Yang, and Y. Liang, "Microwave absorbing properties of composites reinforced by irregular carbon fiber," *Acta Materiae Compositae Sinica*, vol. 26, no. 2, pp. 94–100, 2009.

[7] I. D. G. Ary Subagia, Y. Kim, L. D. Tijing, C. S. Kim, and H. K. Shon, "Effect of stacking sequence on the flexural properties of hybrid composites reinforced with carbon and basalt fibers," *Composites Part B Engineering*, vol. 58, no. 3, pp. 251–258, 2014.

[8] J. Qiu and T. Qiu, "Fabrication and microwave absorption properties of magnetite nanoparticle- carbon nanotube-hollow carbon fiber composites," *Carbon*, vol. 81, no. 1, pp. 20–28, 2015.

[9] X. Wei, H. Cheng, Z. Chu, Z. Chen, and C. Long, "Effect of carbonization temperature on the structure and microwave absorbing properties of hollow carbon fibres," *Ceramics International*, vol. 37, no. 6, pp. 1947–1951, 2011.

[10] T. Ishikawa, *Advances in Inorganic Fibers*, 2005.

[11] Z. Zhang, X. Liu, H. Zhang, and E. Li, "Electromagnetic and microwave absorption properties of carbon fibers coated with carbonyl iron," *Journal of Materials Science Materials in Electronics*, vol. 26, no. 9, pp. 6518–6525, 2015.

[12] J. Li, S. Bi, B. Mei et al., "Effects of three-dimensional reduced graphene oxide coupled with nickel nanoparticles on the microwave absorption of carbon fiber-based composites," *Journal Of Alloys And Compounds*, vol. 717, pp. 205–213, 2017.

[13] X. Chen, X. Wang, L. Li, and S. Qi, "Preparation and microwave absorbing properties of nickel-coated carbon fiber with polyaniline via in situ polymerization," *Journal of Materials Science Materials in Electronics*, vol. 27, no. 6, pp. 5607–5612, 2016.

[14] Y. Shao, W. Lu, H. Chen, J. Q. Xiao, Y. Qiu, and T.-W. Chou, "Flexible ultra-thin Fe_3O_4/MnO_2 core-shell decorated CNT composite with enhanced electromagnetic wave absorption performance," *Composites Part B Engineering*, vol. 144, pp. 111–117, 2018.

[15] Y. Fan, H. Yang, X. Liu, H. Zhu, and G. Zou, "Preparation and study on radar absorbing materials of nickel-coated carbon fiber and flake graphite," *Journal of Alloys & Compounds*, vol. 461, no. 1-2, pp. 490–494, 2008.

[16] K. Zhang, Q. Zhang, X. Gao et al., "Effect of absorbers' composition on the microwave absorbing performance of hollow Fe_3O_4 nanoparticles decorated CNTs/graphene/C composites," *Journal Of Alloys And Compounds*, vol. 748, pp. 706–716, 2018.

[17] L. Yan, C. Hong, B. Sun et al., "In situ growth of core–sheath heterostructural SiC nanowire arrays on carbon fibers and enhanced electromagnetic wave absorption performance," *Acs Applied Materials & Interfaces*, vol. 9, no. 7, pp. 6320–6331, 2017.

[18] D. F. Lii, J.-L. Huang, L.-J. Tsui, and S.-M. Lee, "Formation of BN films on carbon fibers by dip-coating," *Surface & Coatings Technology*, vol. 150, no. 2-3, pp. 269–276, 2002.

[19] A. Rezaie, W. G. Fahrenholtz, and G. E. Hilmas, "Oxidation of zirconium diboride–silicon carbide at 1500°C at a low partial pressure of oxygen," *Journal of the American Ceramic Society*, vol. 89, no. 10, pp. 3240–3245, 2006.

[20] Z. Zhou, C. Lai, L. Zhang et al., "Development of carbon nanofibers from aligned electrospun polyacrylonitrile nanofiber bundles and characterization of their microstructural, electrical, and mechanical properties," *Polymer*, vol. 50, no. 13, pp. 2999–3006, 2009.

[21] J. S. Li, C.-R. Zhang, and B. Li, "Preparation and characterization of boron nitride coatings on carbon fibers from borazine by chemical vapor deposition," *Applied Surface Science*, vol. 257, no. 17, pp. 7752–7757, 2011.

[22] G. M. Shi, S. Lian, G. Song, and J. B. Zhang, "Prepared and microwave-absorption properties of BN coated Ni nanocapsules," *Materials Science Forum*, vol. 663-665, pp. 1252–1255, 2010.

[23] T. Shang, Q. Lu, L. Chao, Y. Qin, Y. Yun, and G. Yun, "Effects of ordered mesoporous structure and La-doping on the microwave absorbing properties of $CoFe_2O_4$," *Applied Surface Science*, vol. 434, pp. 234–242, 2018.

[24] R. Pankajavalli, S. Anthonysamy, K. Ananthasivan, and P. R. V. Rao, "Vapour pressure and standard enthalpy of sublimation of H_3BO_3," *Journal of Nuclear Materials*, vol. 362, no. 1, pp. 128–131, 2007.

[25] H. Onoda, A. Takenaka, K. Kojima, and H. Nariai, "Influence of addition of urea and its related compounds on formation of various neodymium and cerium phosphates," *Materials Chemistry & Physics*, vol. 82, no. 1, pp. 194–198, 2003.

[26] C. Sun, Y. Guo, X. Xu et al., "In situ preparation of carbon/-Fe_3C composite nanofibers with excellent electromagnetic wave absorption properties," *Composites Part A Applied Science & Manufacturing*, vol. 92, pp. 33–41, 2017.

[27] M. Das, A. K. Basu, S. Ghatak, and A. G. Joshi, "Carbothermal synthesis of boron nitride coating on PAN carbon fiber," *Journal of the European Ceramic Society*, vol. 29, no. 10, pp. 2129–2134, 2009.

[28] M. Zhang, Q. C. Liu, Z. F. Zi, Y. Q. Dai, and J. M. Dai, "Magnetic and microwave absorption properties of Ni1−x Zn x Fe2O4 nanocrystalline synthesized by sol-gel method," *Science China Technological Sciences*, vol. 56, no. 1, pp. 13–19, 2012.

[29] W. Zhou, P. Xiao, and Y. Li, "Preparation and study on microwave absorbing materials of boron nitride coated pyrolytic carbon particles," *Applied Surface Science*, vol. 258, no. 22, pp. 8455–8459, 2012.

[30] M. Liu, J. Xiang, Z. P. Wu, J. L. Li, and X. Q. Shen, "Facile preparation and microwave absorption properties of Fe-Co-Ni alloy nanoparticle embedded-carbon nanofibers," *Chinese Journal of Inorganic Chemistry*, vol. 33, no. 1, pp. 57–65, 2017.

[31] W. Lei, F. He, and Y. Wan, "Facile synthesis and electromagnetic wave absorption properties of magnetic carbon fiber coated with Fe-Co alloy by electroplating," *Journal of Alloys & Compounds*, vol. 509, no. 14, pp. 4726–4730, 2011.

[32] Y. Wan, J. Xiao, C. Li, G. Xiong, and H. Luo, "Microwave absorption properties of FeCo-coated carbon fibers with varying morphologies," *Journal of Magnetism & Magnetic Materials*, vol. 399, pp. 252–259, 2016.

[33] Q. L. Sun, L. Sun, Y. Y. Cai et al., "Fe_3O_4-intercalated reduced graphene oxide nanocomposites with enhanced microwave absorption properties," *Ceramics International*, vol. 45, no. 15, pp. 18298–18305, 2019.

[34] "Preparation and microwave absorption property of flexible lightweight magnetic particles-carbon fiber composites#br#," *Journal of Textile Research*, vol. 40, no. 1, pp. 97–102, 2019.

[35] Z. Han, D. Li, H. Wang et al., "Broadband electromagnetic-wave absorption by FeCo/C nanocapsules," *Applied Physics Letters*, vol. 95, no. 2, article 053115, 2009.

[36] J. Xiang, J. Li, X. Zhang, Q. Ye, J. Xu, and X. Shen, "Magnetic carbon nanofibers containing uniformly dispersed Fe/Co/Ni nanoparticles as stable and high-performance electromagnetic wave absorbers," *J.mater. chem. a*, vol. 2, no. 40, pp. 16905–16914, 2014.

[37] X. Sun, J. He, G. Li et al., "Laminated magnetic graphene with enhanced electromagnetic wave absorption properties," *Journal Of Materials Chemistry C*, vol. 1, no. 4, pp. 765–777, 2013.

[38] W. Ye, L. Wei, S. Qilong, Y. Jin, and G. Qiang, "Microwave absorption properties of lightweight and flexible carbon fiber/-magnetic particle composites," *Rsc Advances*, vol. 8, no. 44, pp. 24780–24786, 2018.

[39] N. Dishovsky and M. Grigorova, "On the correlation between electromagnetic waves absorption and electrical conductivity of carbon black filled polyethylenes," *Materials Research Bulletin*, vol. 35, no. 3, pp. 403–409, 2000.

[40] W. Ye, Q. Sun, and G. Zhang, "Effect of heat treatment conditions on properties of carbon-fiber-based electromagnetic-wave-absorbing composites," *Ceramics International*, vol. 45, no. 4, pp. 5093–5099, 2019.

[41] Y. Huang, X. Ding, S. Li, N. Zhang, and J. Wang, "Magnetic reduced graphene oxide nanocomposite as an effective electromagnetic wave absorber and its absorbing mechanism," *Ceramics International*, vol. 42, no. 15, pp. 17116–17122, 2016.